Ninth International Conference on CFD in the Minerals and Process Industries
CSIRO, Melbourne, Australia
10-12 December 2012

MODELLING CONCEPT FOR SUBMERGED ARC FURNACES

Dadan DARMANA[1*], Jan E. OLSEN[1], Kai TANG[2] and Eli RINGDALEN[2]

[1] Sintef Materials and Chemistry, Dept. of Process Technology, Trondheim 7465, NORWAY
[2] Sintef Materials and Chemistry, Dept. of Metallurgy, Trondheim 7465, NORWAY

ABSTRACT

A modelling concept applicable to submerged arc furnaces is presented. The model is based on an Eulerian multi fluid model accounting for granular materials, liquid phases and gas with multiple reacting species. Heat is governed by an applied electric potential distributed by ohmic heating and radiation. The coupled nature of these phenomena makes the process difficult to model properly. A modelling concept has been developed and verified. The model is applied to a pilot scale furnace and tested at full scale. It is shown that transient 3D modelling of the process is feasible.

INTRODUCTION

Silicon is produced industrially by reduction of silicon dioxide (SiO_2) from quarts with carbon from coal and/or coke in submerged arc furnaces by a reaction that in idealized form can be written as Schei (1998):

$$SiO_2 + 2C \rightleftharpoons Si + 2CO \qquad (1)$$

In reality the reaction scheme consist of several reactions and the reaction listed above does not consider any impurities in the raw material. The silicon furnace is described in detail by Schei *et.al.* (1998) and is illustrated in Figure 1. The reactor is heated by dissipation of electric energy passing through the furnace in the form of ohmic heating and electric arching.

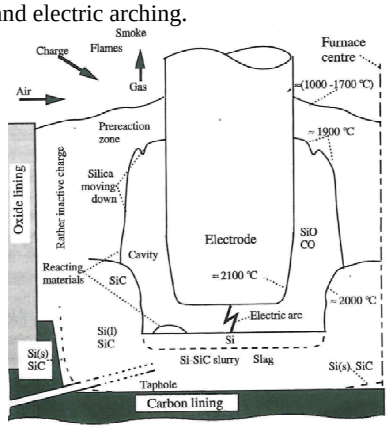

Figure 1: The inner structure of a submerged arc furnace smelting silicon (Schei *et.al.* (1998))

The inner operation of the working furnace is difficult to asses. The combination of high temperature and aggressive chemical environment prove to be challenging for materials probing and measurements to be carried out. For this reason, modelling can be an indispensable tool to help furnace operator or designer to understand and control the process.

Modelling attempts on the process were carried out in the 1990's. They either assumed a 1D-approcah (floor model) or axisymmetric with limited modelling of material flow (Schei, 1982; Schei, 1991, Andersen, 1995a, Andersen, 1995b; Halvorsen, 1993). These simplifications were necessary due to the computing power and numerical routines available at that time. Due the development of high performance computing and more advanced numerical routines, a novel transient 3D modelling concept have been developed to assess the feasibility of modelling the silicon process and other submerged arc furnace processes. It has not been an ambition to develop a trustworthy and validated model.

MODEL DESCRIPTION

The silicon refining process is a complicated process involving various interdependent physical phenomena involving thermodynamics, electricity, hydrodynamics, heat radiation and chemical reactions. This complexity makes the modelling of the process quite challenging. Most of these may be overcome, and the remaining challenges could be solved by adjusting the ambitions of the modelling concept.

Modelling challenges

Time scale

The aforementioned phenomena happen on various time scales ranging from the frequency applied to electricity field to the overall reactor process (i.e. typical tapping and/or stoking frequency). In order to capture the entire time scale, simulations have to resolve the smallest time scale of electricity. This would be prohibitively expensive in terms of computational cost if the goal is to capture a typical process cycle (at least one tapping and/or stoking period).

Phases and Species

The amount of phases and species involved in the silicon reduction process is quite large. Table 1 shows the phases and species matrix used in the modelling concept presented in the following section. In total 5 phases are present: gas, liquid-silica, liquid-silicon, solid and condensate. Furthermore each phase consist of multiple species amounting to 10 species in total. In reality the solid phase should be split in two solid phases; one mineral phase (silica) and one reduction material phase (carbon), but for modelling simplicity they have been described as one phase in the base model. In reality there is also many more species, since all impurities have been neglected.

Copyright © 2012 CSIRO Australia

Table 1: Phases and Species matrix

Gas	Liq. silica	Liq. silicon	Solid	Conden-sate
$SiO(g)$	$SiO_2(l)$	$Si(l)$	$SiC(s)$	$Si(s,l)$
$CO(g)$			$SiO_2(s)$	$SiO_2(s,l)$
$\mathrm{Air}(g)$			$C(s)$	

For each phase one set of governing equations for the hydrodynamics has to be solved. They express conservation of mass, momentum and energy. In addition conservation of N_s species results in N_s - 1 additional transport equations to be solved. Therefore in our constellation, 15 conservation equations, 5 species equations together with the differential equation for the electric potential and the radiation equations need to be solved for each computational cell. This is quite demanding on both CPU and data storage requirement.

Reaction kinetics

It is not possible to account for all reactions in the process. Some have not been identified, and those we know about are already quite numerous. For some of these reactions, there is also a lack of data for the reaction kinetics. It is not feasible to obtain detailed reactions kinetics of all reactions, and even for some of the important ones data are missing.

Hydrodynamics

For the hydrodynamics, the main challenges are related to extreme difference in the properties of the materials present in the reactor. Density varies between one kg/m^3 in gas phase to thousands of kg/m^3 in solid phase while viscosity varies between 10^{-5} kg/ms in gas phase to 10^5 kg/ms in molten silica. Another challenge is caused by the size and shape of the particles in the solid phase. The behaviour of the phase is challenging to model as fluid.

Geometry

The furnace geometry plays an important factor in the modelling work. Pilot-scale silicon reduction furnaces normally consist of one electrode therefor allowing us to model it economically using axis-symmetric simplification. However, an industrial furnace often consist of three electrodes with different electric potential which forces us to model it in full three dimensions at a much higher CPU cost.

Plasma

Plasma modelling is a science by itself. The set of equations describing the dynamics of the plasma physics consist of equations of motion coupled with Maxwell's equations for electromagnetic fields (or Poisson's Equation for electrostatic field) and energy equation. The time scale of the plasma dynamics is also orders of magnitude smaller than the typical process cycles.

Modelling strategy

To answer the aforementioned modelling challenges, a modelling strategy is proposed in this section. The modelling concept is incorporated in the latest version of ANSYS/Fluent version 13 (ANSYS,2011).

The time scale is different for the various phenomena. The frequency of the electric potential is typically 50Hz and thus the time step required to resolve the electric field, Δt_e, can be less than 1 ms. The plasma dynamics is probably described by the same time scale. The typical gas velocities requires a time step for the fluids, Δt_f, around 10 ms. This is roughly the same time scale as the reaction dynamics, Δt_r. Still the smallest time step is associated with the solid phase, Δt_s. Although the solid phase moves slowly, numerically it is necessary to track this phase with a small time step to cover the possibilities of sudden rearrangements in the packed bed. The time step is typically 1 µs, while the process cycle we wish to simulate is typically 1 hr. The order of the time scales is summarized as:

$$\begin{aligned} &\Delta t_s\, O(10^{-6}s) < \Delta t_e\, O(10^{-3}s) < \Delta t_r \\ &\Delta t_r \leq \Delta t_f\, O(10^{-2}s) < \Delta t_p\, O(1h) \end{aligned} \qquad (2)$$

In order to achieve acceptable computational time, a multiple time scale concept is used. In this concept:

- Electrical current is modelled as quasi steady state (electric current change only due to change in phase conductivity and variations in electric potential).
- Simulation runs mainly on fluid time scale at which reactions takes place.
- During fluid time scale, solid phase is assumed to be in static condition and modelled as packed bed.
- When predetermined condition is met, stoking is carried out.
- In the stoking period (smaller) solid time scale is used and solid phase is allowed to move in order to have solid packing reorganization, solid phase is modelled as granular fluidized bed in this period.
- When cavity is refilled and gas from the cavity has been released from the furnace, simulation is switched back to the fluid time step and the solid phase is modeled again as a packed bed and a new cycle starts.

Thus the simulations normally run with a time step capturing the dynamics of the gas flows and the reactions. In the event of stoking or other events causing sudden movements in the particle bed, the time step is reduced to capture these events. This is illustrated in Figure 2. With this feature it is possible to simulate a typical process cycle within reasonable time.

However, it is not possible to capture the plasma dynamics with these restrictions on the time step. This is acceptable since there is no ambition to study that phenomenon in detail. Note that the model needs to realistically account for the heat transfer by the plasma. This needs to be achieved through some effective material parameters, and should not require any smaller time steps than otherwise used.

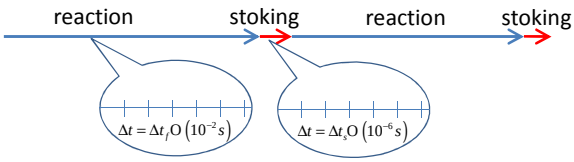

Figure 2: Time step switching strategy to capture different phenomena.

The modelling concept accounts for the solid material (raw material) as a granular phase with special physics such as a maximum packing limit. In addition there are two liquid phases, one gas phase and one condensate phase with species as mentioned above. A set of the reactions assumed to be most significant is accounted for. These reactions are listed in Table 2

Copyright © 2012 CSIRO Australia

Table 2: Relevant Reactions taking into account in the present study

No	Reaction
1.	$SiO(g) + 2C(s) \rightarrow SiC(s) + CO(g)$
2.	$2SiO(g) \rightarrow SiO_2(s,l) + Si(s,l)$
3.	$Si(s,l) \rightarrow Si(l)$
4.	$SiO_2(s) \rightarrow SiO_2(l)$
5.	$SiC(s) + SiO(g) \rightarrow 2Si(l) + CO(g)$
6.	$2SiO_2(l) + SiC(s) \rightarrow 3SiO(g) + CO(g)$
7.	$SiO_2(s,l) \rightarrow SiO_2(l)$
8.	$SiO_2(l) + C(s) \rightarrow SiO(g) + CO(g)$

Reaction 1 is the reaction which reacts SiO gas and carbon into SiC and CO gas. Reaction 2 is the condensation of SiO gas producing SiO_2 and Si condensate. Reaction 3 is phase change from silicon condensate to liquid silicon. Reaction 4 is another phase change from solid silica to liquid silica. Reaction 5 is the reaction between silicon carbide and SiO gas to produce liquid silicon and carbon monoxide gas. Reaction 6 is the reaction between liquid silica and silicon carbide to produce SiO and CO gas. Reaction 7 is another phase change between SiO_2 condensate and SiO_2 liquid. Finally reaction 8 is the reaction between liquid silica and carbon to produce SiO and carbon monoxide gas.

Governing Equations

Conservation of mass and momentum is ensured by the continuity equation and the Navier-Stokes equations. Turbulence is accounted for by the mixture *k - e* model.

For the solid phase (quartz and carbon material) the continuum theory of granular flow is being used. The materials move according the conservation of momentum:

$$\begin{aligned}&\frac{\partial}{\partial t}\left(\rho_s\alpha_s\mathbf{u}_s\right)+\nabla\cdot\left(\rho_s\alpha_s\mathbf{u}_s\mathbf{u}_s\right)\\&=-\alpha_s\nabla P-\nabla p_s+\nabla\cdot\tau_s+\alpha_s\rho_s\mathbf{g}\\&+\sum_{p=1}^{N_p}\left(K_{ps}\left(\mathbf{u}_p-\mathbf{u}_s\right)+\dot{m}_{ps}\mathbf{u}_{ps}-\dot{m}_{sp}\mathbf{u}_{sp}\right)\\&+\left(\mathbf{F}_s+\mathbf{F}_{vm,s}\right)\end{aligned}\tag{3}$$

For granular flows in the compressible regime (i.e. when the solids volume fraction is less than its maximum allowed value), a solids pressure is calculated independently and used for the pressure gradient term ∇p_s shown in Eq.(3). The solids pressure is composed of a kinetic term and a second term due to particle collisions:

$$p_s=\alpha_s\rho_s\Theta_s+2\rho\left(1+e_{ss}\alpha_s^2g_{0,ss}\Theta_s\right)\tag{4}$$

where e_{ss} is the coefficient of restitution for particle collisions $g_{0,ss}$ is the radial distribution function, and Θ_s is the granular temperature determined by solving the following transport equation:

$$\begin{aligned}&\frac{3}{2}\left[\frac{\partial}{\partial t}\left(\rho_s\alpha_s\Theta_s\right)+\nabla\cdot\left(\rho_s\alpha_s\mathbf{u}_s\Theta_s\right)\right]\\&=\left(-p_s\mathbf{I}+\tau_s\right):\nabla\mathbf{u}_s+\nabla\cdot\left(k_{\Theta_s}\nabla\Theta_s\right)\\&-\gamma_{\Theta_s}+\phi_{ps}\end{aligned}\tag{5}$$

where $\left(-p_s\mathbf{I}+\tau_s\right):\nabla\mathbf{u}_s$ is the generation of energy by the solid stress tensor, $k_{\Theta_s}\nabla\Theta_s$ the diffusion of energy, γ_{Θ_s} the collisional dissipation of energy and ϕ_{ps} the energy exchange between the pth fluid and the sth solid phase.

The energy equation is solved for every phase. The governing equation reads as:

$$\begin{aligned}&\frac{\partial}{\partial t}\left(\rho_k\alpha_kh_k\right)+\nabla\cdot\left(\rho_k\alpha_k\mathbf{u}_kh_k\right)\\&=\alpha_k\frac{\partial}{\partial t}p_k+\tau_k:\nabla\mathbf{u}_k-\nabla\cdot\mathbf{q}_k\\&+\sum_{p=1}^{N_p}\left(Q_{pk}\right)+q_k^{\Omega}+S_k^{\Omega}\end{aligned}\tag{6}$$

where $\mathbf{q}_k$ is the heat flux, q_k^{Ω} is the source to ohmic heating described below, S_k^h is a source term that included sources of enthalpy (e.g., due to chemical reaction or radiation), Q_{pk} is the intensity of heat exchange between the p and k phase.

The sensible enthalpy h is calculated as:

$$h=h_{ref}+\int_{T_{ref}}^{T}c_pdT\tag{7}$$

where h_{ref} is the reference enthalpy, T_{ref} is the reference temperature and c_p is the specific heat at constant pressure.

The volumetric rate of energy transfer between phases is assumed to be a function of the temperature difference, i.e.

$$Q_{pk}=h_{pk}\left(T_p-T_k\right)\tag{8}$$

where $h_{pk}\left(=h_{kp}\right)$ is the volumetric coefficient between phase p and phase k. The heat transfer coefficient is related to the p phase Nusselt number, Nu_p as:

$$h_{pk}=\frac{6\kappa_k\alpha_p\alpha_k\mathrm{Nu}_p}{d_p^2}\tag{9}$$

where k_k is the thermal conductivity of the k phase. Fluent provide two Nusselt correlations, Ranz and Marshall commonly use for fluid-fluid heat transfer and Gunn for granular flows (i.e. solid-fluid) heat transfer.

<u>Electric potential and Ohmic heating</u>

The electric current continuity equation is given in terms of the electric potential j as follow:

$$\nabla\cdot\left(\sigma_m\nabla\varphi\right)=0\tag{10}$$

where, s_m is the mixture electrical conductivity.

The current density vector $\left(\mathbf{J}\right)$ is related to the electric potential distribution as follows:

$$\mathbf{J}=-\sigma_m\nabla\varphi\tag{11}$$

The total heat generated due to the dissipation of electric energy is calculated using Ohm's law:

Copyright © 2012 CSIRO Australia

$$q_m^{\Omega} = \frac{\mathbf{J} \cdot \mathbf{J}}{\sigma_m} \tag{12}$$

The electric current continuity equation shown in Eq. (10) is solved using mixture User-Defined Scalar (UDS) equation with the transient and convective term turned off. The mixture electrical conductivity is calculated based the phase value with volume weighted average as:

$$\sigma_m = \sum_{p=1}^{N_p} \alpha_p \sigma_p \tag{13}$$

The heat source attributed to phase k is determined from the mixture heat generated q_m using volume weighted as:

$$q_k^{\Omega} = \alpha_k q_m \tag{14}$$

The heat radiation from a heat source is modelled via Discrete Ordinates (DO) radiation model. The discrete ordinates radiation model solves the radiative transfer equation (RTE) for a finite number of discrete solving angles, each associated with a vector direction *s* fixed in the global Cartesian system.

The DO model requires input parameters such as absorption coefficient, scattering phase function and refractive index. The suggested default value from Ansys is used in the present study.

Species i in phase k is represented by mass fraction Y_k^i. The governing equation for multiphase species transport equation

$$\frac{\partial}{\partial t}\left(\rho_k \alpha_k Y_k^i\right) + \nabla \cdot \left(\rho_k \alpha_k \mathbf{u}_k Y_k^i + \alpha_k \mathbf{J}_k^i\right) = \alpha_k R_k^i + \alpha_k S_k^i + \sum_{p=1}^{N_p}\left(\dot{m}_{p^i,k^j} - \dot{m}_{k^j,p^i}\right) + \mathbf{R} \tag{15}$$

where R_k^i is the net rate of production of homogeneous species i by chemical reaction for phase k, $\dot{m}_{p_i^i,k^j}$ is the mass transfer source between species i and j from phase k to p, and **R** is the heterogeneous reaction rate. In addition S_k^i is the rate of production form user defined source. $\mathbf{J}_k^i$ is the diffusion flux of species i resides in phase k.

Reaction kinetics based on heat flux received by material is used in the present study (i.e. if sufficient energy is present, the reactions occur instantaneously).

Table 3: Reaction kinetics

No	Rate [mole/m^{2}s]	Reaction condition
1.	$k_1 = A\, e^{E/RT}$	$\Delta G^0 < 0\ \forall\ T$
2.	$k_2 = q_2 / \Delta H_2$	$\Delta G^0 < 0\ \forall\ T < 2110\ K$
3.	$k_3 = q_3 / \Delta H_3$	$\Delta G^0 < 0\ \forall\ T < 1691\ K$
4.	$k_4 = q_4 / \Delta H_4$	$\Delta G^0 < 0\ \forall\ T < 1996\ K$
5.	$k_5 = q_5 / \Delta H_5$	$\Delta G^0 < 0\ \forall\ T < 2216\ K$
6.	$k_6 = q_6 / \Delta H_6$	$\Delta G^0 < 0\ \forall\ T < 2135\ K$
7.	$k_7 = q_7 / \Delta H_7$	$\Delta G^0 < 0\ \forall\ T < 1996\ K$
8.	$k_8 = q_8 / \Delta H_8$	$\Delta G^0 < 0\ \forall\ T < 2016\ K$

In Table 3, ΔH represents the change of enthalpy while ΔG represents the change of entropy. The heat flux q appears in the reaction rate is calculated based on solid temperature and reaction equilibrium temperature as:

$$q = h\left(T_s - T_{eq}\right) \tag{16}$$

where T_{eq} is the temperature limit in which reaction can happen

SIMULATIONS

The governing equations presented above are solved using the finite volume technique implemented in commercial CFD software Fluent version 13 (of ANSYS Inc., USA) (ANSYS (2011)). Most of the governing equations are solved using the standard solver available from the software while the electric potential equation shown in Eq. **Error! Reference source not found.** is solved using the User Defined Scalar (UDS) solver. Furthermore, user customized model such as momentum transfer, heat transfer and reaction kinetic were written using User Defined Functions (UDF) written in the C programming language.

The following models were turned on during simulations:

- Multiphase – Eulerian
- Energy
- Viscous – Standard k-epsilon, Standard Wall Fn, Mixture
- Radiation – Discrete Ordinates
- Species – Species Transport, Reactions

Typical time needed to calculate 1 process interval between two stoking process consisting of 1400 s real time is 24 hours wall time using 8 parallel processors.

Numerical Scheme

All governing equations are solved using second order quadratic upwind (QUICK) scheme. Explicit volume fraction formulation is used which allow the software to select time step based on CFL criteria. The CFL criteria used in the present study is 0.5, with maximum time step of 0.5 s.

Geometry and boundary conditions

A pilot scale furnace is modelled in the present study. The geometry of the furnace can be seen in Figure 3. Note that the electrode tip is modelled with rounded corners since sharp corners promote a numerical singularity. To reduce calculation time during model development, the geometry is modelled as axis-symmetric. The geometry is discretised into total of 580 computational cells. Wall boundary conditions are used for solid boundary while pressure outlet is used on the top of the furnace to allow gas phase to leave or enter the computational domain. Electric potential equation is modelled with boundary of +100 V at the electrode surface and -50 at the bottom of the furnace while zero gradients are imposed on other boundary. For the energy equation, thermal convection boundary with heat transfer coefficient of 1000 w/m^2-K and free stream temperature of 300 K is applied on the side wall boundary while zero flux thermal boundary is applied on the bottom furnace.

Initial conditions

Simulations are started with set of initial condition. The solid phase is filled up to 60 % of the total height of the furnace with volume fraction of 0.62. The solid phase consists of mixture of 75% SiO_2 and 25% C with patch of 1% SiC is set below the electrode tip to speed up initial

Copyright © 2012 CSIRO Australia

reaction. The gas phase occupies the rest of the volume consisting of air. The phases not present initially such as condensate, liquid SiO_2 and liquid Si, is set to have volume fraction of 1×10^{-6}. Temperature for all phases is set to 300K. The scalar quantity representing the electric potential is set initially at 0. Mixture turbulent kinetic energy is set to 1 m^2/s^2 and mixture turbulent dissipation rate 1 m^2/s^3. All phases are set to be initially at rest while the solid granular temperature is set to 0.0001 m^2/s^2.

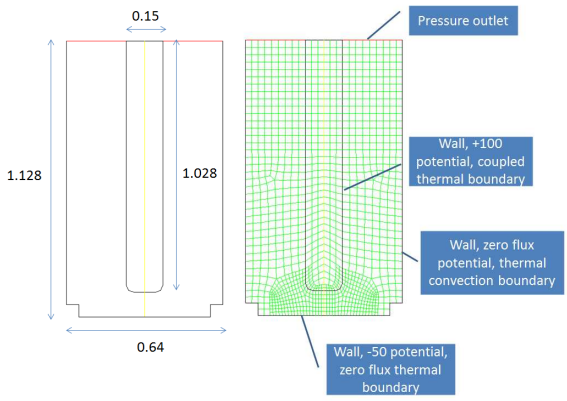

Figure 3: Geometry (in meter), computational mesh and boundary conditions

RESULTS

Electric potential and ohmic heating

Snapshots of the electric potential field can be seen on Figure 4 (left). Due to extremely high velocity of the electrical current travel in space, the electric potential equation is assumed to be always in equilibrium in every time step. Variation in space due to the mixture electrical conductivity as consequences of inhomogeneous materials composition is however accounted for.

Based on the electrical potential field, source term for energy equation is calculated. As the source term is based on the gradient of the electric potential field, it is obvious that in the present case, the region next to the electrode tip is exposed to most of the heat source as can be seen on Figure 4 (right).

The ohmic heat source is distribute to each phases using volume weighing. Figure 5 shows snapshots of the temperature field from two different time instance for solid and gas phase. As can be seen the gas phase reach the maximum temperature almost in no time however at the end due to heat transfer both phases reaching equilibrium temperature with each other. Not that in the present study, all temperature fields is capped at maximum 2500 K to prevent instability in the reaction rate calculations.

Cavity formation

One of the key important features of the silicon arc furnace reactor is the presence of a void cavity next to the electrode tip (see Figure 1). In the present model the cavity is formed naturally when solid materials next to the electrode tip is consumed either due to melting or reaction with other materials.

Figure 6 shows how the cavity is formed in the present simulation. Starting from the electrode tip, the solid phase is gradually consumed (represented by decreasing solid volume fraction locally). The process is continued as solid phase is continually consumed resulting bigger void cavity. When the cavity formation is reaching the outer region of the hot zone, the process is slowed down as there is not enough heat to sustain the cavity formation process.

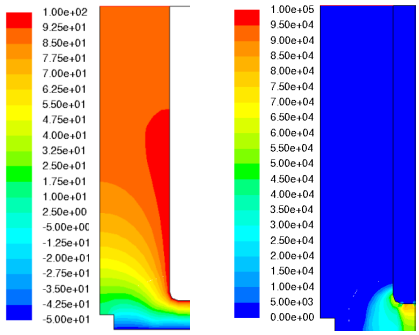

Figure 4: Snapshots of electric potential field [V](left) and ohmic heating source [W/m3] (right)

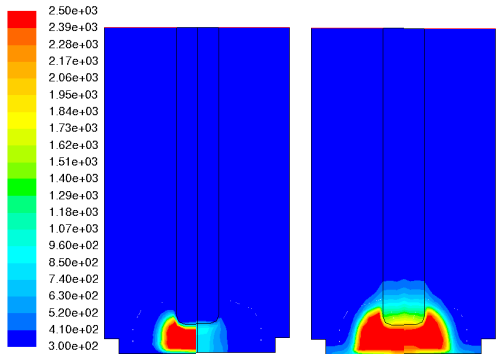

Figure 5: Snapshots of temperature field [K] at *t*=15 (left) and 1000 s (right). The left half part of each picture shows gas phase temperature field while the right solid phase.

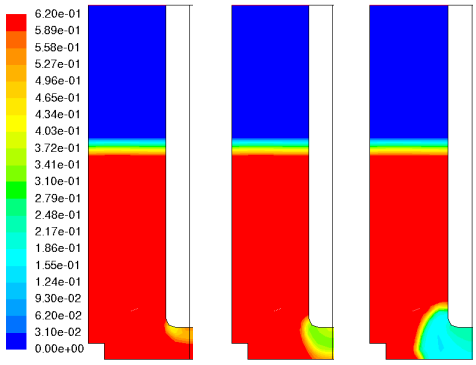

Figure 6: Snapshots of solid phase volume fraction respectively from left to right at *t*=120, 185 and 675 s showing the formation of void cavity in the reactor.

Chemical reactions

Chemical reactions depend very much on the availability of heat and reactant(s). The reaction path is rather complicated, but can be simplified as follow in order to give better understanding. The reaction begins with reaction 4 in which silica melting into liquid. Depending on the availability of silicon carbide and the zone temperature, liquid silica can react following reaction 6 or

Copyright © 2012 CSIRO Australia

8 to produce SiO gas. SiO gas in turn reacts either with carbon according to reaction 1, condensed according to reaction 2 or react with silicon carbide according to reaction 5 depending on temperature. Finally when the temperature is sufficiently high, the condensate phase will melt according to reaction 3 and 7.

Figure 7 show example of instantaneous rate for all reactions taking into account in the present study. As can be seen reactions 1, 5, 6 and 8 occurs mainly on the hot zone inside the cavity while reaction 3, 4 and 7 happens on the cavity wall. Finally, the condensation process represented by reaction 8 take places in colder region slightly away from the cavity wall.

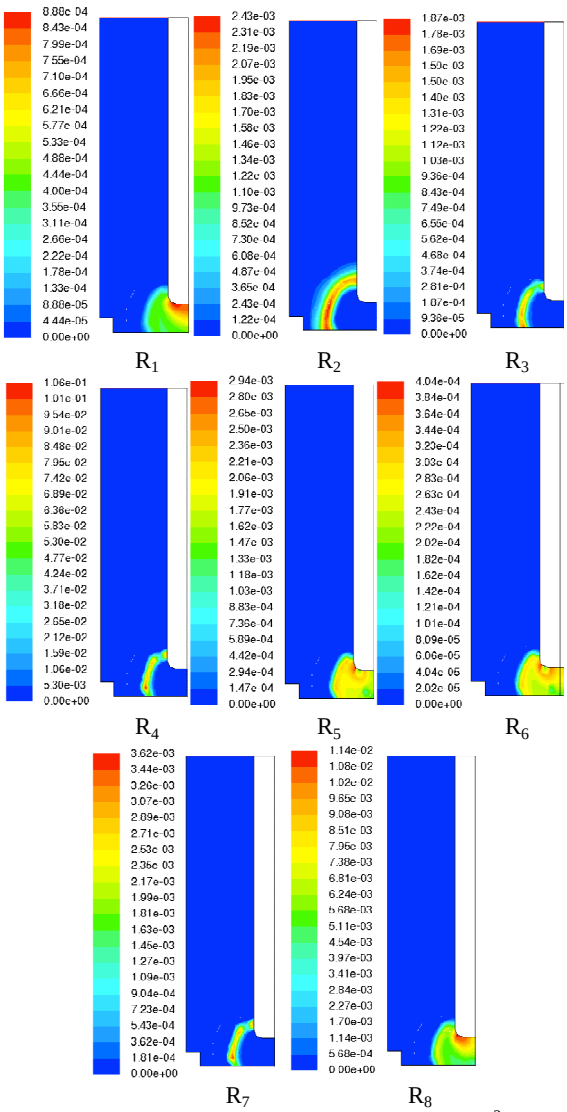

Figure 7: Instantaneous reaction rates [kgmol/m^3-s] for the eight reactions at t=500 s

This information gives detailed indications of where each reaction occurs and the corresponding reaction rate which is of high importance when investigating the limiting reaction which prohibits reaching optimum conversion rate.

Material distribution

Due to the various chemical reactions taking place in the process, materials are going to be redistributed. Figure 8 shows instantaneous volume fraction for the 5 phases taking into account in the present simulation after the process has run for about 1000 s. As can be seen at this time instance, void cavity has taken shape. Liquid silica (due to its sticky nature in liquid form) is attached to the remaining solid materials still present in the hot zone. The condensate material (formed from the condensation of SiO gas) is clearly present at the cavity wall region. Finally the liquid silicon formed in the hot zone is dripping to the base of the reactor. Not that the variation of the hydrodynamics behaviour of liquid silica and liquid silicon is achieved by incorporating different interphase drag correlation between the liquid phases and solid.

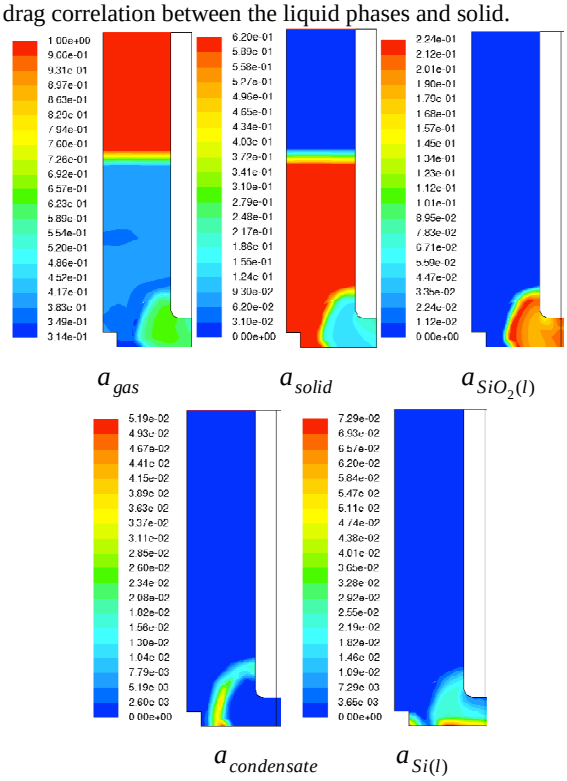

Figure 8: Instantaneous phases volume fraction [-] at t=1000 s.

Species evolution

The evolution of the total mass for each materials present at any given time inside reactor can be easily extracted by doing simple integration for the entire computational cells. Figure 9 shows the example of the evolution of carbon, silicon, silica and silicon carbide materials resulting from the current model.

For the first 100 s, nothing much happen to the materials composition as the reactor is still heating up to the reacting temperature. After the reaction temperature is reached, reactions start. Both carbon and silica are continuously consumed by the reaction. Silicon carbide which was initially added to the reactor is also consumed by the reaction; however after about 400 s it starts to be accumulated again.

Production of silicon starts approximately 100 s after the start of the process. The steep curve at the beginning indicates fast reaction process producing significant amount of silicon. The rate however gradually decreases in time indicating that reactants required to produce silicon probably have been depleted and a stoking process is

Copyright © 2012 CSIRO Australia

needed to replenish the area near electrode tip with fresh materials.

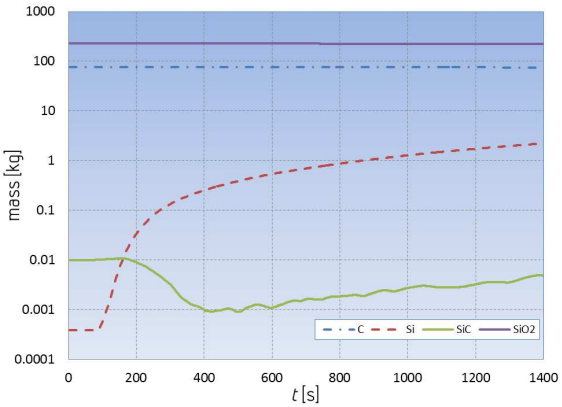

Figure 9: Species evolution over time during interval between two stoking process.

Stoking process

When materials next to electrode tip have been entirely consumed, a stoking process is needed. In the present model the stoking process is carried out by allowing the solid phase to move, effectively switching from a packed bed to a fluidized bed model. Furthermore, numerical time step has to be reduced several order of magnitude in order to capture rapid structural change in the reactor which normally occurs within 1 to 2 s time interval.

Figure 10 shows how the stoking process is simulated by the present model. As can be seen after the stoking process is initiated, the gas pocket starts to rise to the surface. Fresh materials from the side wall region of the reactor sink to the lower reactor part, refilling the cavity region below the electrode. After about 2 s, the stoking process finished and the simulation can be continued by switching the solid phase back to packed bed mode and increasing the time step again to the reaction rate time step.

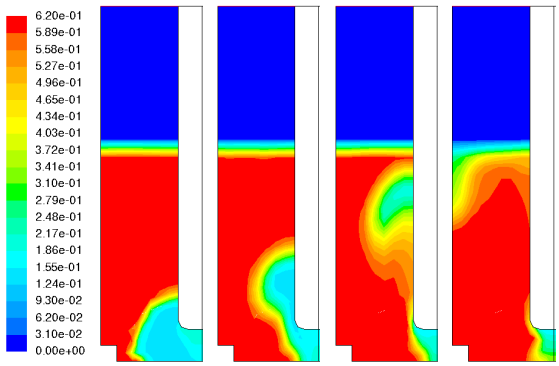

Figure 10: Solid phases volume fraction [-] during stoking process, from left to right at 0, 0.5, 1.0 and .1.8 s after the stoking process started.

Full scale 3D simulation

The modelling concept has also been tested on a full scale furnace with 3D simulation. These furnaces are typically 10 meters in diameter with three electrodes and a 3-phase AC power supply. For the 3D full scale model, a mesh with circa 26000 cells was applied. The computational time increased to 4-5 days for a typical process interval. A snapshot of the ohmic heating source is seen in Figure 11.

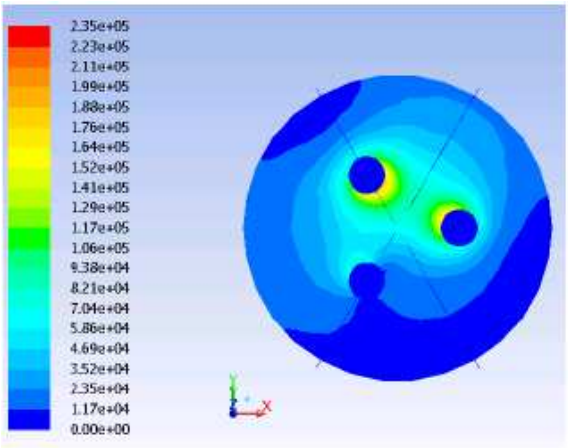

Figure 11: Snapshot of ohmic heat source in a full scale furnace simulation

CONCLUSION

It is not the intention of the present study to build a perfect model for submerged arc furnace. Instead this should be considered as a first step in understanding various elements required to model the furnace and the results that can be expected by conducting simulation of such a complex system. In the present study, we discovered that large amount of input data such as detailed reactions kinetics and material properties are still unaccounted for, thus a dedicated study to provide the data is required. However, the study showed that computer technology and numerical algorithms are capable of processing the input required to simulate the process. The CPU cost is high, but acceptable for industrial simulations. Thus it is feasible to develop a CFD model based on the proposed concept for silicon furnaces and other submerged arc furnaces.

REFERENCES

ANDERSEN, B., (1995a), “Dynamical model for the high-temperature part of the carbothermic silicon metal process”, *INFACON 7.FFF (The Norwegian Ferroalloy Research Organization, SINTEF)*, Trondheim, 1995

ANDERSEN, B., (1995b) “Process model for carbothermic production of silicon metal”. PhD thesis, Norwegian University of Science and Technology, Dept. Metalurgy

ANSYS Inc (2011), ANSYS 13.0 user guide.

HALVORSEN, S.A., DOWNING, J.H., and , SCHEI,A. (1993) “A unidimensional model dynamic model for the (ferro) silicon process”. *Electric Furnace Conf* (1992), Proc 45-59

SCHEI, A. and LARSEN, K., (1982), “A stoichiometric model of the ferrosilicon process”, *Electric Furnace Conf (1981)*, Proc **39,** 301-309.

SCHEI, A., HALVORSEN, S.A., and TVEIT, H. (1998), “Production of High Silicon Alloys”, Tapir forlag, Norway.

SCHEI, A. and HALVORSEN,S.A., (1991), “A stoichiometric model of the silicon process”. *Ketil Motzfeldt Symposium*, Institute of Inorganic Chemistry, The Technical University of Norway, 41-56

Copyright © 2012 CSIRO Australia